RSC Advances

ROYAL SOCIETY OF CHEMISTRY

www.rsc.org/advances

Design of fluorescence aptaswitch based on the aptamer modulated nano-surface impact on the fluorescence particles

Atul Sharma [a, b], Akhtar Hayat [c, a], Rupesh Kumar Mishra [a, d], Gaëlle Catanante [a], Shakir Ahmad Shahid [e], Sunil Bhand [a], Jean Louis Marty [a, *]

[a] BAE Laboratoire, Université de Perpignan Via Domitia, 52 Avenue Paul Alduy, 66860 Perpignan 13 Cedex, France.

[b] Biosensor Lab, Department of Chemistry, BITS, Pilani- K. K. Birla Goa Campus, Zuarinagar 403726, 16 Goa, India.

[c] Interdisciplinary Research Centre in Biomedical Materials (IRCBM), COMSATS Institute of 18 Information Technology (CIIT), Lahore 54000, Pakistan.

[d] Department of Biosciences and Biotechnology, Banasthali University, Rajasthan, 304022, India.

[e] Department of Chemistry, University of Sargodha, Sargodha 40100, Pakistan

[*]Corresponding Author:

Jean Louis MARTY

Laboratoire BAE

Université de Perpignan Via Domitia

Bâtiment S, 52 avenue Paul Alduy

66860 Perpignan cedex – France

Ph: +33 (0) 4 68 66 22 54, Fax: +33 (0) 4 68 66 22 23

Email: jlmarty@univ-perp.fr

Abstract

The concept of DNA based stabilization of nanostructures to enhance the surface reactivity has been focus of great interest in the design of colorimetric aptaswitches. Whereas, colorimetric methodologies have limited sensitivity, this concept is rarely considered for other sensing approaches such as those based on the fluorescence detection. In this paper, we have investigated the impact of reversible assembly of single strand DNA aptamer on nanoparticles surface chemistry, involving target tuneable electrostatic and steric repulsion phenomena for fluorescence based detection of molecular interaction. In the same context, literature reported fluorescence based aptamer assays are prone to certain limitations such as complicated labelling chemistry, less conjugation yield, low binding affinity and elevated cost per assay. Alternatively, our designed aptaswitch capitalizes on the surface chemistry of nanoparticles to quench the response of fluorescence particles, eliminating the need of bioconjugation with fluorophore. As a proof of concept, the proposed methodology was used for the detection of ochratoxin A with TiO_2 nanoparticles as representative nanomaterial. We expect that this concept may pave a new way to probe aptamer- target binding event, since any nanomaterials with fluorescence quenching characteristics can be regulated in the same manner.

Keywords: Surface chemistry; DNA stabilization; aptamer fluorescence assays; universal platform; OTA detection

Introduction

Since the discovery of DNA-functionalized gold nanoparticles conjugates in 1996,[1,2] many nanomaterials have been utilized to design DNA structure switchable nanosensors based on their plasmon resonance properties.[3] These DNA/aptamer based switches are mainly based on the materials such as gold nanoparticles,[4] silver nanoparticles,[5] quantum dots,[6] magnetic nanoparticles,[7] and dye-doped silica nanoparticles.[8] As bulk materials are devoid of a band gap, nanomaterials must be extremely small to exhibit their distinct and intrinsic properties. In general, a colloidal dispersion of nanoparticles exhibits well defined redox activity, while aggregated nanoparticles pose negligible surface activities.[9] Based on this observation, the concept of DNA based stabilization of nanostructures to enhance the surface reactivity has been focus of great interest in the design of colorimetric aptaswitches.[10] However, these methodologies are limited to colorimetric assays with rare reports on other assays such as those based on the fluorescence detection. In this paper, we have investigated for the first time impact of reversible assembly of single strand DNA aptamer on nanoparticles surface chemistry, involving target tunable electrostatic and steric repulsion phenomena for fluorescence based detection of molecular interaction. Recent literature has witnessed immense interest in the exploration of nanomaterials with fluorescence quenching characteristics for various types of applications. One of the attractive areas in this field of research was to integrate fluorescence quenching properties of nanomaterials in designing easy to use and simple aptamer based fluorescence assays to replace the conventional fluorescence detection methodologies. In this context, many nanomaterials have been investigated to develop novel designs of fluorescence aptasensors for various target analytes. However, these literatures reported fluorescence quenching assays mainly rely on the conjugation of aptamer with fluorophore or dye molecules.[11,12]

The single fluorophore attachment to ss-aptamer/DNA strand decreases the sensitivity of analytical method. A critical assumption is that conformational transition of aptamer from loose random coils to a compact tertiary structure (G-quadruplex ternary complex) might alter the electronic environment of attached fluorophore, which causes significant loss in signal intensity.[13] The low fluorescence enhancement on target analyte binding and less sensitivity, limits their real time applications. Moreover, most of the fluorophores have fluorescent lifetimes in seconds and require specific storage conditions to stabilize their fluorescent response. The difficulty in selection of fluorophore, decreased stability, dual labeling and complicated conjugation chemistry make fluorescent signaling aptaswitching platforms more expensive and unsuitable for on-site analysis.[14] Therefore, the above strategies are not easy to generalize for the development of new methods.

Therefore, it is highly desirable to explore novel concepts in fluorescent based detection methodologies. In this work, we have designed an aptaswitch that capitalizes on the surface chemistry of nanoparticles to quench the response of fluorescence particles, eliminating the need of bioconjugation with fluorophore. The unbound fluorescence particles have been used to replace the commonly used labeling fluorophore or dyes. The high surface to volume ratio of fluorescence particles has resulted in very elevated fluorescence response, enabling the very sensitive detection of target analyte.[15] To the best of our knowledge, this is the first report that correlates the surface chemistry of nanomaterials to quench the response of fluorescence particles, and subsequently integration them in the design of fluorescence aptaswitches. As a proof of concept, the proposed methodology was employed to design aptaswitch for the detection of ochratoxin A (OTA) as a model analyte with TiO_2 nanoparticles as representative nanomaterial. OTA was selected as a target analyte due to its presence in common food stuffs such as alcoholic beverages (beer and wines), cereal grains, dried fruits, coffee and coffee products. OTA posses highly toxic and potential carcinogenic

effects such as nephrotoxic, hepatotoxic, teratogenic and immunotoxicity.[16] According to the European Union, some regulatory limits to control the level of OTA in food stuff (5 or 10 μgkg^{-1}) and beverages (2 μgkg^{-1}) has been introduced (EC No. 123/2005).

However, we assumed that this novel concept in fluorescence aptaswitches may offer a new methodology for sensitive and specific detection of a wide spectrum of analytes for medical, environmental and the electronic applications, since any aptamer-target binding event- in principle can be translated to conformational transition and can be detected via fluorescence quenching mechanism. Moreover, this approach can be very easily extended to other literature reported nanomaterials with fluorescence quenching characteristics to design fluorescence aptaswitches.

2. Materials and methods

2.1. Materials and reagents

The aptamer of OTA was synthesized and purified by Eurogentec (France). The specific sequences of an anti-OTA aptamer is shown below: 5' GAT CGG GTG TGG GTG GCG TAA AGG GAG CAT CGG ACA-3'.[17]

TiO_2 nanoparticles with the diameters of 25 nm were synthesized and provided by PROMES Laboratory, UPVD-Perpignan, France. Fluorophore carboxylate modified particles (FCM) 0.1 µm (350/440) were procured from Life Technologies (USA). HEPES sodium salt was purchased from Fisher Scientific (USA). All other chemical magnesium chloride ($MgCl_2$), potassium chloride (KCl) and sodium chloride (NaCl) of analytical grade were procured from Sigma-Aldrich (France). OTA, derived from (*Aspergillus ochraceus*) was purchased from Sigma Aldrich (France). Ochratoxin B (OTB), derived from (*Aspergillus ochraceus*) was procured from Santa Cruz Biotechnology, Germany. For selectivity studies, N-acetyl-$_L$-phenylalanine (NAP) and warfarin was obtained from Sigma–Aldrich (USA).

The aptamer solutions prepared in HBB binding buffer (HBB, pH 7.4) containing 5 mM $MgCl_2$, 60 mM NaCl and 1.35 mM KCl was dissolved in the deionized Milli-Q water (Millipore, Bedford, MA, USA). The FCM working stock solution was prepared in HBB and subsequently diluted. Quenching efficiency of TiO_2 was evaluated in HBB. For preparation of standards, first OTA was dissolved in methanol (1 mg/mL) and then diluted in HBB. Similarly, OTB standards were prepared for selectivity measurements.

2.2. Instrumentation

A fluorescence imaging system (in-house) consisting of ultraviolet light source coupled with a light excluding compartment, a lens, digital camera and computer was developed for elucidation of assay principle. The obtained image is decomposed into its red, green and blue component (RGB components) and analyzed by computer. The fluorescent measurements (excitation 355 nm; emission 460 nm) were carried out using Fluoroskan Ascent FL 2.6 (Thermo Scientific-Finland) equipped with Ascent software version 2.6 for fluorimetric measurement providing fixed value of fluorescence measurement. The UV-visible spectral measurements were performed on UV- spectrophotometer (UV-1800, USA) equipped with TCC controller to measure the absorption characteristics of aptamer-TiO_2 complex. All fluorescence measurements were performed in standard 96 black microwell plates obtained from Thermo Fisher Scientific, Roskilde, Denmark. Aptamer pre-treatment was done (preheated at 85 °C then 4 °C for 5 min) on thermocycler mastercycler (Eppendorf, Le Pecq, France) before use.

2.3. UV Characterization

The UV-visible spectral measurements were performed to characterize the interaction and the formation of aptamer-TiO_2 complex using UV-spectrophotometer equipped with TCC controller. The UV absorbance of aptamer stabilized TiO_2 nanoparticle with 250 nM aptamer

was measured. The solution was mixed well before each UV-visible measurement and spectrum recorded in the range of 220-400 nm.

2.4. Quenching measurement

Quenching efficiency of TiO_2 nanoparticles was evaluated before and after stabilization with target specific aptamer. In brief, 10 µL of TiO_2 (2.5 to 1000 µg/mL, in microwell) and 10 µL of FCM (100 µg/mL) were properly mixed with 180 µL of HBB. Fluorescence measurements were performed at excitation 355 nm; emission 460 nm. Secondly, 10 µL of aptamer (250 nM in microwell) and 10 µL of TiO_2 at an optimized concentration (300 µg/mL) were mixed with 170 µL of HBB and incubated for 1 h. After the incubation, the FCM (100 µg/mL) was added to aptamer stabilized TiO_2 nanoparticles and quenching measurements were carried out within 30 seconds after FCM addition. Control measurements were performed with FCM keeping the concentration (100 µg/mL) and reaction volume same (200 µL).

2.5. Fluorescence aptamer assay

Fluorescence quenching based aptamer assay was performed by addition of 10 µL of TiO_2 and aptamer at optimal ratio and mixed with 160 µL of HBB followed by 1 h incubation. After incubation, 10 µL volumes of different OTA concentration were added in the respective microwells and again incubated for different time (unless optimized for 1 hr). Finally, 10 µL of FCM (100 µg/mL) was added in each microwell and mixed properly. Quenching measurements were carried out within 30 second after FCM mixing on Fluoroskan Ascent FL 2.6 plate reader at excitation 355 nm; emission 460 nm. Similarly, control measurements were performed without the addition of OTA and keeping other experimental conditions same. Quenching efficiency was calculated from following equation

Q (%) = [1- F_o/F], where F_o and F were the fluorescence intensity in the absence and presence of analyte.[18]

2.6. Preparation of Beer sample

The beer sample (0.5%) was purchased from local market in Perpignan, France. The presence of fluorescent compound in the beer sample may lead to the false signal response. Thus, beer samples were prepared according to a previously described method with slight modification.[19] In brief, the known concentration of OTA was spiked in beer sample and degassed for 30 min to avoid rapid foaming and pH adjusted to 7.4. The spiked beer sample was filtered through 0.45 μm Minisart non-pyrogenic filters (Sartorius Stedim Biotech, USA). Finally, the subsequent dilutions were made with an unspiked beer sample to obtain the different concentration of OTA (0.017, 0.125 and 1.0 μM) in assay volume.

3. Results and Discussion

3.1. Fluorescence quenching assay principle

The designed strategy for fluorescence quenching based aptaswitch sensing platform is illustrated in Fig. 1. In the proposed design of aptaswitch, the high fluorescence intensity of fluorescence particles (FCM) is quenched by TiO_2 nanoparticles as shown in Fig. 1 (a). The large semiconductor band gap behavior of TiO_2 and electrostatic interaction of Ti-O bond between TiO_2-fluorescent probes was attributed to the fluorescence quenching mechanism through the acceptance of electrons from FCM nanoparticles.[20,21] Electrostatic adsorption of ss-aptamer on TiO_2, led to the stabilization of TiO_2 nanoparticles due to formation of TiO_2-aptamer complex. The physical adsorption and electrostatic interaction between the aptamer and TiO_2 nanoparticles surface resulting in stabilization of nanoparticles.

The uniform dispersion of aptamer stabilized TiO_2 particles is responsible for maximum quenching due to enhancement in surface activity as shown in Fig. 1 (b). In the presence of

target analyte, the target induced conformational change in aptamer assembly, leading to desorption of aptamer from nanoparticles surface, which results in the formation of tertiary complex (antiparallel G-quadruplex complex) and subsequently recovery of quenched fluorescence as depicted in Fig. 1 (b). By monitoring the degree of fluorescence recovered among unstabilized and stabilized TiO_2 nanoparticles corresponds to the concentration of target molecule, a calibration curve was performed over the varying concentration of target analyte.

Figure 1

3.2. Fluorescence imaging and UV characteristics

In presence of aptamer stabilized TiO_2 nanoparticle, the fluorescence intensity of fluorescent probe (FCM) is decreased to minimum due to electrostatic interaction between Ti-O bonds. This is strong evidence of fluorescence quenching attributed to the acceptance of electrons from excited fluorescent probe molecules as shown in Fig. 2a (i) and (ii). On addition of target, the target triggered conformational changes in reversible assembly of aptamer weaken the interaction between fluorescent probe and TiO_2, resulting in the recovery of fluorescence response as depicted in Fig. 2a (iii). The recorded fluorescence images were further decomposed into individual RGB component and analyzed using in house developed fluorescence imaging system. The fluorescence magnitude of blue component of FCM decreases in presence of TiO_2, which is a strong indication of fluorescence quenching. As shown in Fig. 2a (iii), on addition of OTA, an increase in value of blue component shows the presence of fluorescence recovery. The obtained results were summarized in the Table 1.

Similarly, the UV spectral measurements were used to characterize the incidents as shown in Fig. 2b. Target specific aptamer showed an absorption maxima at 256 nm (curve b), whereas the TiO_2 did not exhibits UV absorption at the same wavelength (curve a).

Stabilization of nanoparticles showed an enhancement in UV absorption at 256 nm without change in the peak position (curve c and d). This typical characteristic of absorption spectrum shows the adsorption of aptamer on TiO_2 surface, which could be due to the electrostatic interaction between aptamer and TiO_2.[22] As a control experiment, un-stabilized TiO_2 nanoparticles did not exhibit UV absorption at same wavelength (curve a). The UV absorbance results were summarized in Supplementary Table 1.

Figure 2a and 2b, Table 1

3.3. Optimization of the experimental parameters

Experimental parameters, which could affect the quenching based aptamer assay, were optimized. The TiO_2 concentration ranging from 2.5 to 1000 μg/mL were investigated. The relative fluorescence intensity decreased with increase in TiO_2 concentration confirming the fluorescence quenching ability of TiO_2 nanoparticles as shown in Fig. 3a. No increase in quenching was observed with further increase in concentration, thus 300 μg/mL concentration was selected for further experiments. Variation in surface charge is a critical factor which may cause aggregation of TiO_2 nanoparticles at high pH and alter the quenching efficiency.[23] The pH range of buffer from 6.8 to 8.2 was evaluated to obtain the maximum response. At high pH value, the change in surface charge results in agglomeration of TiO_2 nanoparticles which results in decrease in quenching efficiency as shown in Fig. 3b. Dilution factor may also alter the fluorescence response, thus experiments at different assay volume were performed as depicted in Fig. 3c. Increase in assay volume decrease this signal ratio, thus an optimum assay volume of 200 μL was used.

Optimization of aptamer concentration is the critical factor for stabilization of nanoparticles and detection of target molecule. A decrease in fluorescence intensity was observed with increase in aptamer concentration from 10-750 nM as depicted in Fig. 3d. The

increased in quenching efficiency was attributed to the increased stability of TiO_2 nanoparticles, indicating the formation of aptamer-TiO_2 adsorption complex and uniform dispersion. However, the higher concentration of biomolecule increases the signal intensity but decreases the sensitivity of affinity based assay due to increase in background signal, thus the optimized concentration of aptamer was used in further experimentation.[24] Because phosphate and other anionic buffer can be adsorbed by TiO_2 nanoparticles and may cause the artifacts in aptamer adsorption, thus we use HBB in most of our experiments. The effect of pH from 6.8 to 8.2 was also investigated using stabilized TiO_2 nanoparticles. The pH of binding buffer could significantly affect the adsorption kinetics and aptamer-TiO_2 stability.[23,25] Maximum quenching was obtained at pH 7.4 with 250 nM of aptamer as shown in Fig. S1.

Due to changes in the surface charge, nanoparticles may undergo aggregation or render the electrostatic interaction thus resulting a decrease in fluorescence quenching.[26] The unmodified TiO_2 nanoparticles carries the negative surface charge in HBB at pH 7.4, thus the effect of salt was screened to overcome the electrostatic repulsion and obtain maximum aptamer adsorption on TiO_2 surface.[25] As demonstrated in Fig. S2, the percent relative fluorescence intensity decreased with increase in concentration of Na^+ salt (10-60 mM). Fig. S2 clearly suggested that at much higher concentration of Na^+ salt (90 mM), the percent relative fluorescence intensity further increased, which strongly suggested the non-specific adsorption of Na^+ on TiO_2 surface, which decreases the fluorescence quenching. Similarly, the divalent metals which are responsible for binding affinity of aptamer to OTA and acting as ionic bridge enhances the electrostatic interaction in between the TiO_2 and aptamer. As shown in Fig. S3, the percent relative fluorescence intensity is decreased with increase in Mg^{2+} salts from 1-5 mM, thus further experimentation were carried out under optimized conditions. The results in figure S4 and S5 suggested that the optimal time for maximum

quenching response was nearly 1 h, as after this time interval, the quenching efficiency was decreased due to undesired agglomeration or multilayer formation of aptamer on nanosurface.

Figure 3

3.4. Quantitative measurement of OTA (calibration curve)

Under optimal experimental conditions, the calibration curve was performed for different OTA concentrations in buffer solutions. In Fig. 4a, the recovered fluorescence intensities were plotted as a function of OTA concentration from 0.017 to 5.0 μM in HBB, pH 7.4. Encouragingly, it was found that the FL intensity recovered continuously with increasing concentrations of OTA due to the high binding affinity of OTA to form the anti-OTA aptamer-G-quadruplex complex. The calibration curve was fitted using the linear equation with a line of the equation as $y = 41.67 x + 6.604$ (coefficient of correlation of $R^2 = 0.9913$, n=4) with linearity from 0.017 to 5.0 μM OTA. The limit of detection (LOD) was calculated as the concentration of analyte corresponds to the recovered fluorescence signal at 3 times standard deviation of the blank sample (without OTA). The LOD was found to be 1.35 nM of OTA.

The proposed method was presented with better analytical merits of figures as compared to earlier reported methods based fluorescence and colorimetric signal generation for OTA detection as summarized in Table 2. This detection strategy exhibiting higher sensitivity than our previous reported work, whereas the fluorescein labeled anti-OTA aptamer (recognition element and fluorophore) and TiO_2 nanoparticles (quencher) was employed for detection of OTA.[34] The higher sensitivity of present aptaswitch was attributed to the stabilization of aptamer modulated nano surfaces, which offer an advantage of uniform dispersion and stability. Moreover, our previous strategy was based on the conjugation of aptamer with fluorophore molecules, however, this work capitalizes on the surface chemistry of

nanoparticles to quench the response of fluorescence particles, eliminating the need of bioconjugation with fluorophore, overwhelming the problems associated with nanomaterials based fluorescence quenching assays.

Table 2

3.5. Selectivity studies of the developed assay

The selectivity is an important parameter in evaluating the performance of an aptamer assay. The specificity of the proposed aptamer assay was evaluated at varying concentration of 0.25, 1.0 and 5.0 μM of structurally similar non-specific analogues OTB, N-acetyl-L-phenylalanine (NAP) and warfarin. As shown in Fig. 4b, the addition of target molecule (OTA) exhibits the significant increase in the recovered fluorescence intensity; however other analogue did not induced apparent fluorescence response at same concentration. The fluorescence response obtained with other analogue were negligible in comparison to OTA (blue bar), therefore this aptamer was highly specific to OTA. The obtained response were found to be more accurate with less than 10 % (n=3) at three different concentrations as shown in supplementary Table ST2.

Figure 4

3.7. Analytical merits of assay

The repeatability and reproducibility of the developed aptamer assay platform were evaluated by performing the intra or inter assay precision. The precision studies were performed with fixed concentration of OTA (0.25 μM) under optimized experimental conditions. Control measurements were performed for each assay without OTA. The recovered fluorescence intensity was calculated from the response obtained with/ without OTA samples. The intra assay precision with % R.S.D (n=3) of 5.04 was calculated for

triplicate measurements of OTA. Similarly, the % R.S.D. (n=3) from 1.53 to 6.79 was calculated for inter assay precision. The obtained results from intra and inter assay precision prove the applicability of sensing platform for real sample analysis and results are summarized in Table 3.

3.6. Recovery and real sample analysis

In order to validate the performance of assay, the practical application of the proposed sensing platform was evaluated for detection of OTA in beer sample. Due to incidence of high occurrence of OTA in alcoholic beverages, the proposed aptaswitch platform was used as model for analysis of beer sample.[16] Recovery studies were performed in OTA spiked beer sample at different concentrations of OTA including 0.017, 0.125 and 1.0 μM. The obtained recoveries were calculated based on the fluorescence response recovered in the buffer and spiked beer sample. As shown in Table 3, the obtained recoveries were in the good agreements (96.79- 99.04% (n=3)) to the spiked concentrations with maximum relative standard deviation (%RSD) of 6.02 for the triplicate measurements. The obtained results suggested the acceptability of quenching based aptamer assay, which could be further employed for detection of OTA in other matrices.

Table 3

4. Conclusions

In conclusion, this work reported a universal fluorescence aptasensing design based on the DNA modulated surface chemistry of nanoparticles. This is the first time that modulation in the surface chemistry of nanomaterials has been explored to quench the response of fluorescence particles. The proposed concept was employed to construct fluorescence aptaswitch to probe molecular binding events. As no special characteristic of attaching ssDNA are required, any ssDNA-target binding event can in principle be translated to

conformational transition and can be detected with fluorescence output signal. This novel assay method is simple in design, avoiding oligonucleotide labelling or nanoparticles modification, and signal is based on the impact of modulated surface properties of particle on fluorescence particles rather than labelled fluorophore or dye as is the case with most of the other quenching based aptamer assay. Taken together above advantages, we believe that this aptaswitch concept may offer a new methodology for sensitive and specific detection of a wide spectrum of analytes for medical, environmental and the electronic applications.

Acknowledgments

The present work is financially supported by NATO SfP-Bio-Optical Sensors, Project No. 984637 SPS NUKR.SFPP. Atul Sharma would like to thank EUPHRATES program for ERASMUS Mundus doctoral fellowship.

Conflict of interest

Authors declare that they do not have any conflict of interest.

Reference:

1. P. Alivisatos, K. P. Johnsson, X. Peng, T. E. Wilson, C. J. Loweth, M. P. Bruchez and P. G. Schultz, *Nature*, 1996, **382**, 609-611.
2. C. A. Mirkin, R. L. Letsinger, R. C. Mucic and J. J. Storhoff, *Nature*, 1996, **382**, 607-609.
3. J. Wang, L. Wang, X. Liu, Z. Liang, S. Song, W. Li, G. Li and C. Fan, Advanced Materials, 2007, **19**, 3943-3946.
4. J. Liu and Y. Lu, *Angewandte Chemie International Edition*, 2006, **45**, 90-94.
5. J.-S. Lee, A. K. R. Lytton-Jean, S. J. Hurst and C. A. Mirkin, *Nano Letters*, 2007, **7**, 2112-2115.
6. C.-Y. Zhang, H.-C. Yeh, M. T. Kuroki and T.-H. Wang, *Nat Mater*, 2005, **4**, 826-831.
7. S. Bamrungsap, T. Chen, M. I. Shukoor, Z. Chen, K. Sefah, Y. Chen and W. Tan, *ACS Nano*, 2012, **6**, 3974-3981.
8. X. Zhao, R. Tapec-Dytioco and W. Tan, *Journal of the American Chemical Society*, 2003, **125**, 11474-11475.
9. A. Hayat and S. Andreescu, *Analytical chemistry*, 2013, **85**, 10028-10032.
10. G. Bulbul, A. Hayat and S. Andreescu, *Advanced healthcare materials*, 2016, **5**, 822-828.
11. S. Wu, N. Duan, X. Ma, Y. Xia, H. Wang, Z. Wang and Q. Zhang, *Analytical chemistry*, 2012, **84**, 6263-6270.
12. Z. S. Qian, X. Y. Shan, L. J. Chai, J. J. Ma, J. R. Chen and H. Feng, *Nanoscale*, 2014, **6**, 5671–5674.
13. R. Nutiu and Y. Li, *Chemistry (Weinheim an der Bergstrasse, Germany)*, 2004, **10**, 1868-1876.
14. S. Song, L. Wang, J. Li, C. Fan and J. Zhao, *TrAC Trends in Analytical Chemistry*, 2008, **27**, 108-117.
15. A. Hayat, R. K. Mishra, G. Catanante and J. L. Marty, *Analytical and bioanalytical chemistry*, 2015, **407**, 7815-7822.
16. L. Monaci and F. Palmisano, *Anal. Bioanal. Chem*. 2004, **378,** 96–103.
17. J. A. Cruz-Aguado and G. Penner, *Journal of Agricultural and Food Chemistry*, 2008, **56**, 10456-10461.

18. M. Balcioglu, M. Rana, N. Robertson and M. V. Yigit, *ACS Applied Materials & Interfaces*, 2014, **6**, 12100-12110.
19. A. Visconti, M. Pascale and G. Centonze, *Journal of Chromatography A*, 2000, **888**, 321-326.
20. C. Wang, C. Liu, Y. Wang and T. Shen, *Journal of colloid and interface science*, 1998, **197**, 126-132.
21. H. P. Wu, T. L. Cheng and W. L. Tseng, *Langmuir: the ACS journal of surfaces and colloids*, 2007, **23**, 7880-7885.
22. A. Kathiravan and R. Renganathan, *Polyhedron*, 2009, **28**, 1374-1378.
23. D. L. Liao, G. S. Wu and B. Q. Liao, *Colloids and Surfaces A: Physicochemical and Engineering Aspects*, 2009, **348**, 270-275.
24. A. Hayat, L. Barthelmebs and J.-L. Marty, *Analytica Chimica Acta*, 2011, **690**, 248-252.
25. X. Zhang, F. Wang, B. Liu, E. Y. Kelly, M. R. Servos and J. Liu, *Langmuir : the ACS journal of surfaces and colloids*, 2014, **30**, 839-845.
26. T. Amano, T. Toyooka and Y. Ibuki, *Science of the Total Environment*, 2010, **408**, 480-485.
27. L. Sheng, J. Ren, Y. Miao, J. Wang and E. Wang, *Biosensors & bioelectronics*, 2011, **26**, 3494-3499.
28. C. Yang, Y. Wang, J. L. Marty and X. Yang, *Biosensors & bioelectronics*, 2011, **26**, 2724-2727.
29. Z. Guo, J. Ren, J. Wang and E. Wang, *Talanta*, 2011, **85**, 2517-2521.
30. J. Chen, Z. Fang, J. Liu and L. Zeng, *Food Control*, 2012, **25**, 555-560.
31. Z. Lv, A. Chen, J. Liu, Z. Guan, Y. Zhou, S. Xu, S. Yang and C. Li, *PLoS ONE*, 2014, **9**, e85968.
32. Y. Wei, J. Zhang, X. Wang and Y. Duan, *Biosensors and Bioelectronics*, 2015, **65**, 16-22.
33. Y. Luan, J. Chen, C. Li, G. Xie, H. Fu, Z. Ma and A. Lu, *Toxins*, 2015, **7**, 4883.
34. A. Sharma, A. Hayat, R. Mishra, G. Catanante, S. Bhand and J. Marty, *Toxins*, 2015, **7**, 3771.
35. L. Lv, C. Cui, C. Liang, W. Quan, S. Wang and Z. Guo, *Food Control*, 2016, **60**, 296-301.

Legend of Tables:

Table 1: Fluorescence magnitude value of blue components

Table 2: Comparison of proposed aptaswitch platform with earlier reported method for OTA detection

Table 3: Recovery and analytical performance of spiked OTA in beer sample using developed aptaswitch platform

Legends of Figures:

Figure 1: Schematic representation of structure switching signaling aptaswitch based on fluorescence quenching principle for detection of target analyte

Figure 2a: Fluorescence images of (i) OTA (in buffer), (ii) FCM (in buffer), (iii) FCM + TiO_2 (in buffer), (iv) FCM+ aptamer-TiO_2 (in buffer) and (v) FCM+ aptamer-TiO_2 + OTA (in buffer).

Figure 2b: UV spectrum of aptamer at different condition in HBB (a) TiO_2, (b) aptamer, (c) and (d) aptamer + TiO_2

Figure 3a: Optimization of TiO_2 concentration against FCM (100 μg/mL) for structure signaling aptaswitch platform in HBB.

Figure 3b: Optimization of pH condition (6.8 to 8.2) for development of structure signaling aptaswitch platform in HBB at optimal TiO_2 concentration (300 μg/mL).

Figure 3c: Optimization of assay volume for development of structure signaling aptaswitch platform in HBB, pH 7.4.

Figure 3d: Optimization of aptamer concentration for development of structure signaling aptaswitch platform in HBB, pH 7.4.

Figure 4a: Standard calibration curve obtained based on the recovered fluorescence intensity against OTA concentration. Error bar were obtained from four parallel experiments (n=4).

Figure 4b: Specificity studies of developed aptaswitch platform for OTA detection against OTB in the sample (n=3). Error bar were obtained from four parallel experiments (n=3).

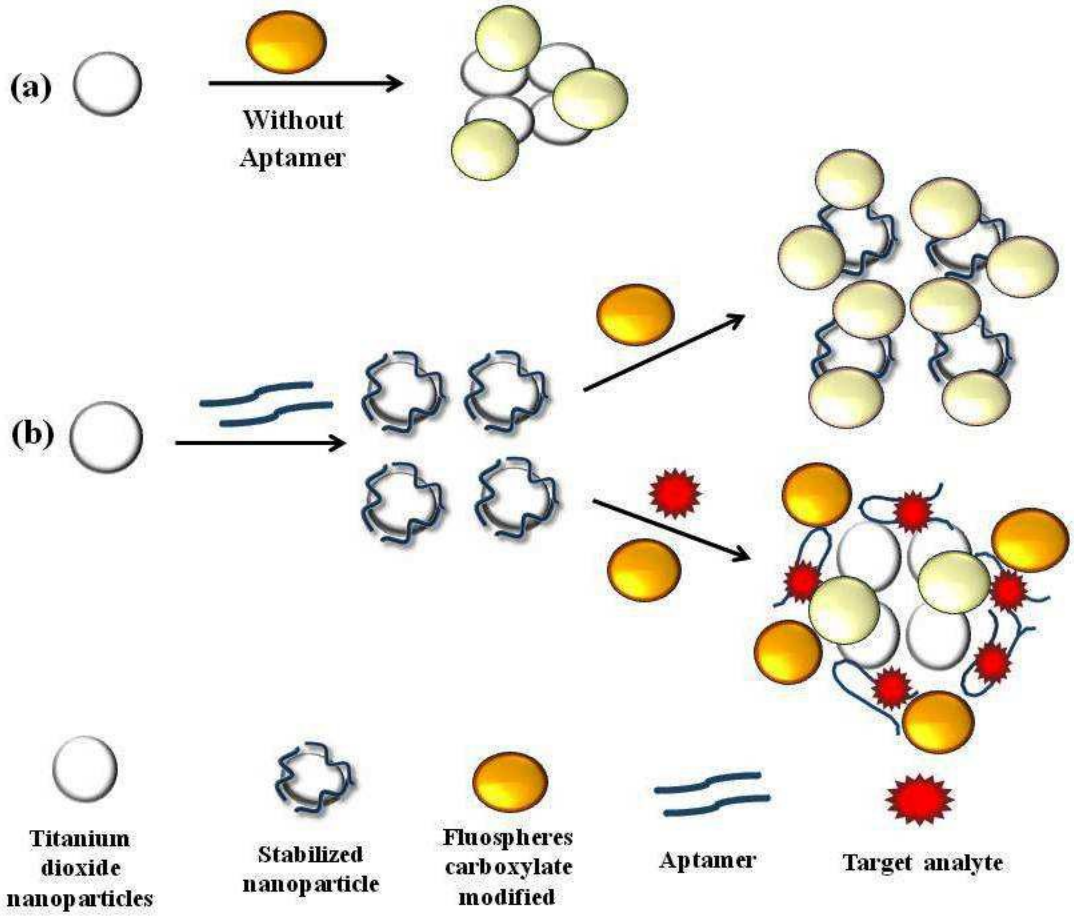

Figure 1

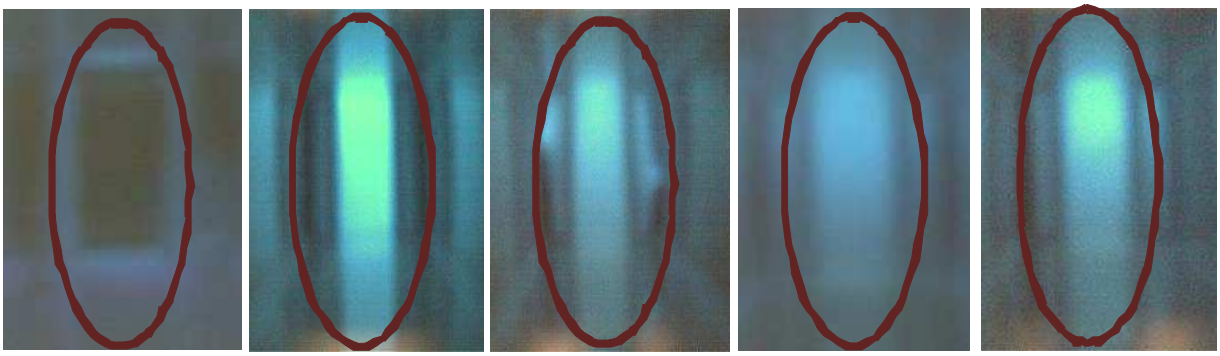

(i) (ii) (iii) (iv) (v)

2 (a)

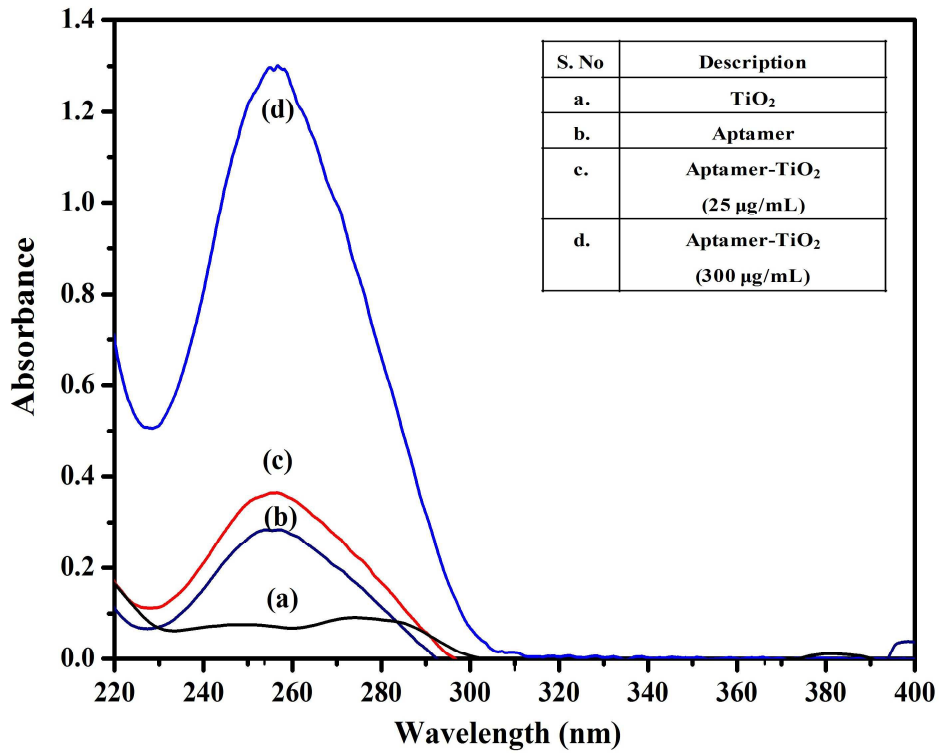

2 (b)

Figure 2

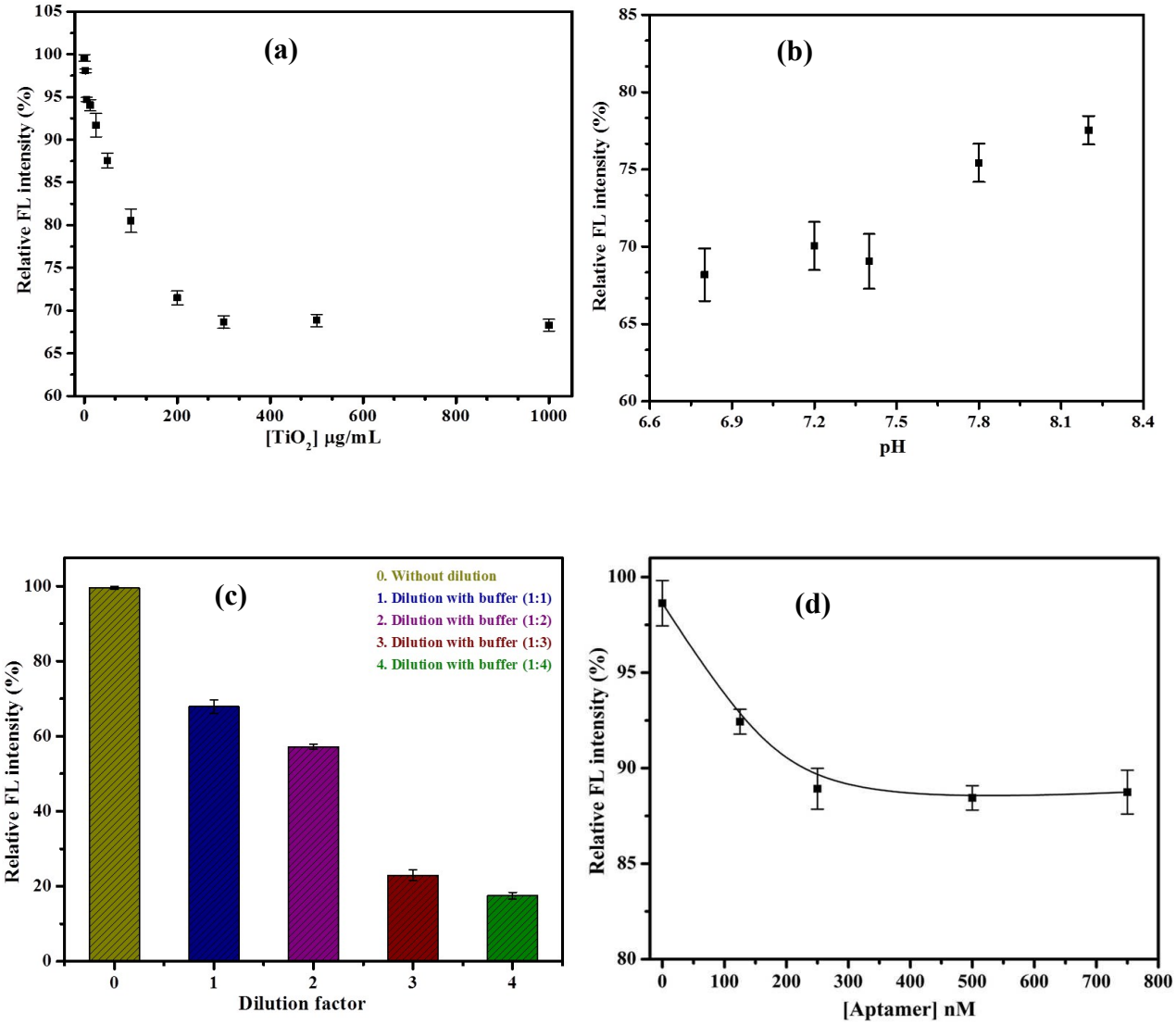

Figure 3

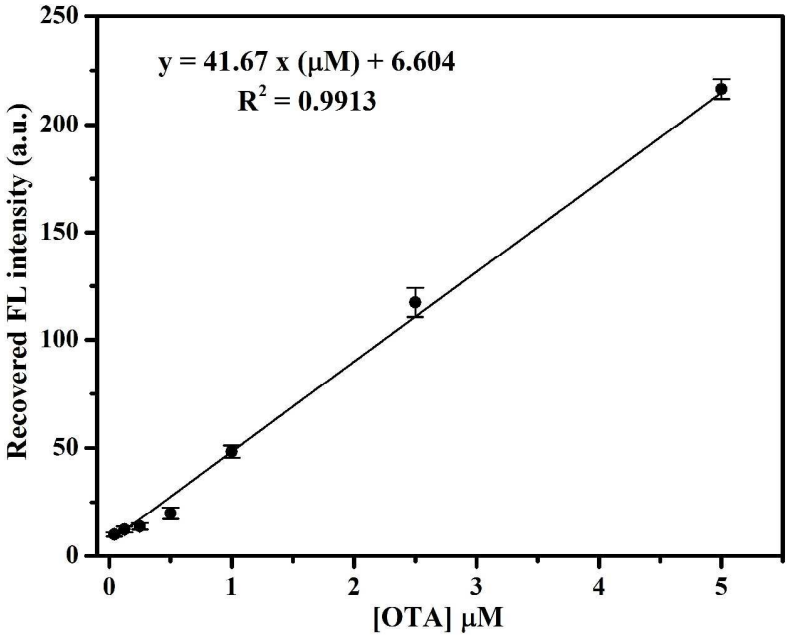

4 (a)

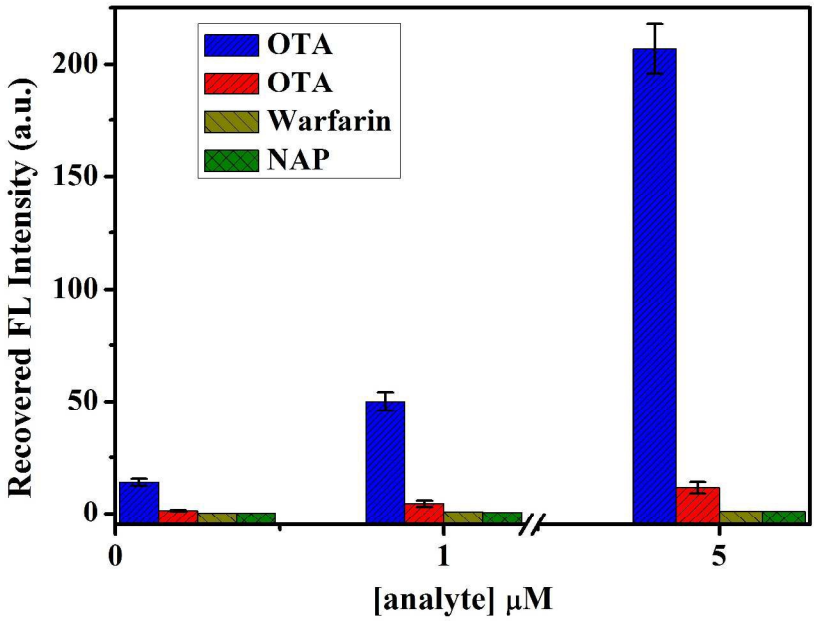

4 (b)

Figure 4

Table 1: Fluorescence magnitude value of blue components

S. No.	Description	Blue component value
1.	OTA + buffer	20
2.	FCM* + buffer	160
3.	FCM* + TiO_2 + buffer	115
4.	FCM + aptamer-TiO_2 + buffer	89
5.	FCM + aptamer-TiO_2 + OTA + buffer	120

*FCM- Fluorophore carboxylate modified particles, OTA- ochratoxin A

Table 2: Comparison of proposed aptasensing platform with earlier reported aptamer assay for OTA detection

S. No.	Materials	Methods	Linearity	LOD	Ref.
1.	**Graphene oxide**				
	1. Bare graphene	Fluorescence	2-35 μM	1.9 μM	[27]
	2. PVP coated graphene oxide		50-500 nM	21.8 nM	
2.	**Gold nanoparticles**	Colorimetric	20-625 nM	20 nM	[28]
3.	**Single walled carbon nanotubes (SWNTs)**	Fluorescence	25-200 nM	24.1 nM	[29]
4.	**Molecular beacons**	Fluorescence	2.5- 250 nM	1.98 nM	[30]
5.	**Label free détection**	Fluorescence	2.5 nM - 2.5 μM	2.5 nM	[31]
6.	**Nanographite**				
	1. Bare nanographite	Fluorescence	2-50 μM	2 μM	[32]
	2. DNase catalyzed amplification		20-400 nM	20 nM	
7.	**Gold nanoparticle**	Colorimetric	12 nM – 0.12 μM	22 nM	[33]
8.	**Titanium dioxide nanoparticles**	Fluorescence quenching	1.5 nM - 20 μM	1.5 nM	[34]
9.	**Single-walled carbon nanohorn (SWCNHs)**	Fluorescence	20-500 nM	17.2 nM	[35]
10.	**Fluorescence quenching based aptamer assay**	Fluorescence Quenching	17 nM - 5 μM	1.35 nM	**Present work**

Table 3: Recovery and analytical performance of spiked OTA in beer sample using developed aptasensing platform

Recovery performance of fluorescence aptamer assay in beer sample					
Beer Sample	**OTA added [µM]**	**OTA found [µM]**	**Mean ± S.D. (n=3)**	**% R.S.D.**	**% Recovery**
1.	0.0170	0.0166	0.0166 ± 0.0010	6.02	97.65
2.	0.1250	0.1210	0.1210 ± 0.0032	2.48	96.79
3.	1.0000	0.9940	0.9940 ± 0.0292	2.91	99.40

Interday precision analysis				
Days	**OTA concentration [µM]**	**Recovered FL intensity (a.u.)**	**Mean ± S.D.**	**% R.S.D.**
Day-1	0.25	13.73	13.73 ± 0.87	6.33
Day-2	0.25	14.13	14.13 ± 0.96	6.79
Day-3	0.25	13.65	13.65 ± 0.21	1.53

Intraday precision analysis					
OTA concentration [µM]	**Recovered FL intensity (a.u.)**			**Mean ± S.D.**	**% R.S.D.**
	Response-1	**Response-2**	**Response-3**		
0.25	13.5	14.8	14.7	14.33 ± 0.79	5.04

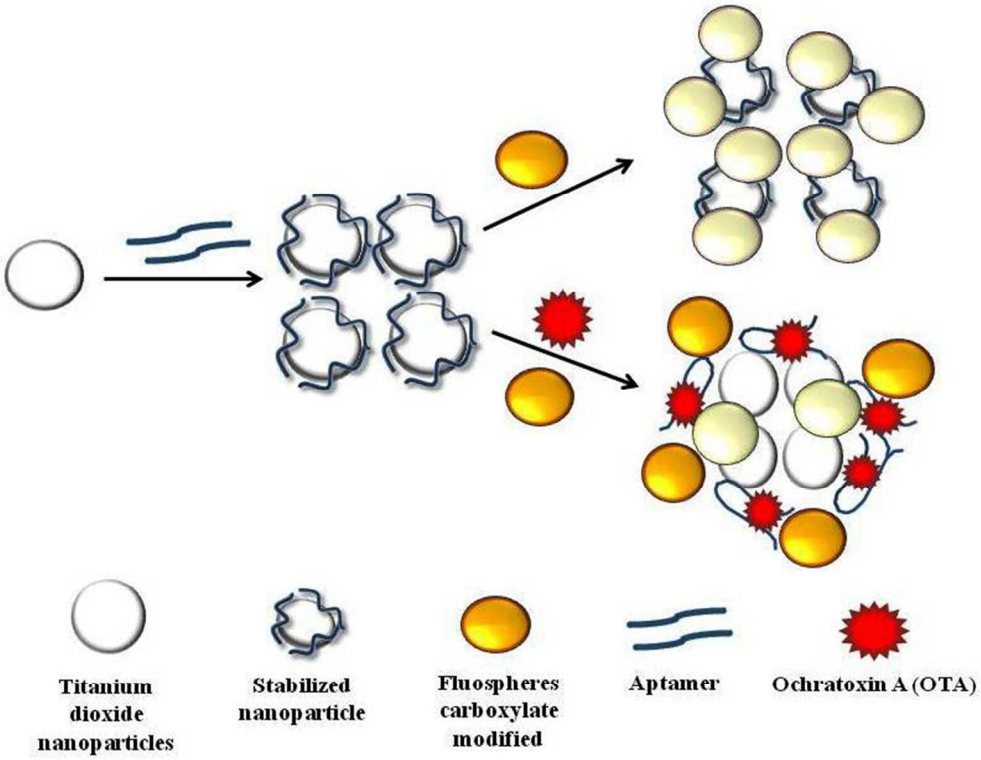

213x167mm (96 x 96 DPI)